Proceedings of the International Conference on Oxide Materials for Electronic Engineering, May 29–June 2, 2017, Lviv

Analysis of Observed Voltage Oscillations in Silver Doped High Temperature Superconductor YBCO

A. Altinkok[a,*], M. Olutas[b], H. Yetis[b], A. Kiliç[b] and K. Kiliç[b]

[a]Giresun University, Engineering Faculty, Department of Electrical and Electronics, 28200 Giresun, Turkey

[b]Abant Izzet Baysal University, Department of Physics, Turgut Gulez Research Laboratory 14280 Bolu, Turkey

The effect of square wave current was investigated by the voltage–time (V–t curves) measurements at various external magnetic fields and periods (P) in silver doped YBCO. The general sinusoidal behavior of V–t curves was mainly interpreted as a dynamic competition between driving and pinning forces. It is observed that as the period of square wave current is increased, the amplitude of oscillation is also increased. The observed oscillations in the voltage was fitted by an common sinusoidal equation $V(t) \sim \sin(\omega t + \varphi)$. It is also found that there is different phase angle φ values for each cycle. Fast Fourier transform measurements is applied to oscillation period (P_I) of the square wave current. The results give us that a physical mechanism is related with charge density waves. Intrinsically, in Ag doped YBCO, the pinned flux line system evokes the general behavior of charge density waves. Due to properties of the converting the square wave current to sinusoidal voltage oscillations, Ag doped YBCO sample can behave as double-integrator for the defined period, amplitude of square wave current and magnetic field values in time.

DOI: 10.12693/APhysPolA.133.1030

PACS/topics: 74.25.F–, 74.72.–h

1. Introduction

Experimental results brought out that the flux lines by variation of the current cause different motional redistribution in the superconductors [1–6]. Fast Fourier transform (FFT) measurements were done by square wave currents which showed that the driven current is re-organized to vortices [1]. D'anna et al. [1] suggested that the instabilities observed in detwinned single crystalline sample of YBCO arises from the entry surface barriers which affects the coherent motion of the vortices entry or exit along the surfaces of the single crystal. Kwok et al. [6] reported peculiar voltage oscillations in time to ac sinusoidal type driving current below the melting/freezing line of single crystalline sample of YBCO. They attributed the oscillatory instability in the HTSC sample to the rivalry between the forces of the driving and pinning together with relaxation effects and the long range spatial correlations in the vortex solid. Gordeev et al. [2, 7] and Rassau et al. [8] showed that the observation of coherent voltage oscillations having low frequency depends strongly on temporal asymmetry of the drive and also its magnitude. The unusual instabilities were explained in terms of transitions between ordered and disordered states of vortex matter. In order to observe the periodic oscillations in response, the asymmetric current pulses are essential feature in producing such instabilities. In our case, one of the major conditions to observe periodic voltage oscillations in the V–t curves is to apply symmetric square wave current to the sample [3, 5, 9].

*corresponding author; e-mail: atilgan.altinkok@giresun.edu.tr

2. Experimental

Silver doped YBCO samples were prepared by the same solid state reaction method which was used in our previous works [3, 10, 11] to add 1% weight silver of amount of Cu into YBCO samples.

The measurements were recorded by PC controlled an IEEE-488 interface card. A temperature stability better than 0.01 K was maintained during the measurements (Oxford Instruments, ITC-503 temperature controller) in the He closed cycle cryostat system. Keithley-2182A and Keithley 6221 were used to measure the sample voltage and apply the current, respectively. The external magnetic field was applied by an electromagnet (Oxford Instruments, N100 electromagnet) in the experiments. The critical current density (J_c) of an Ag-doped YBCO-123 polycrystalline bulk sample, whose results are presented in this study, is ≈ 40 A/cm^2 at $T = 88$ K by using the 1 μV/cm criterion. The critical temperature T_c of the sample at zero magnetic field is found as ≈ 92 K. The normal state resistivity ($T = 300$ K) (ρ_n) of the YBCO/Ag sample at room temperature is less than 0.1 mΩcm. This value is much smaller than that of undoped polycrystalline YBCO sample with $\rho_n \approx 1.5$ mΩcm and reflects directly the effect of Ag doping on transport properties of YBCO ceramics.

The time evolution of the sample voltage (V–t curves) was measured by applying square wave (SW) current (with long period (P) and different amplitudes) at zero magnetic field ($H = 0$) and by applying magnetic field (H). For our purpose, the commercial current source (Keithley-6221) and the nanovoltmeter (Keithley-2182A) are adequate to produce such SW currents, and to read low voltage levels with high precision. Just after the driving current is applied, we started to record the sample

voltage developing along the sample. Thus, all details of the time evolution of the sample voltage including temporary effects become possible.

The voltage oscillations in the YBCO/Ag sample can be described by an empirical equation given in the below,

$$V(t) = A + B\sin(\omega t + \varphi), \quad (1)$$

where A and B are the constants, w is the frequency and φ is the phase angle.

3. Results and discussion

Figure 1a–c illustrates time evolution of the voltage of the sample, at $T = 88$ K for a SW current of amplitude, 20 mA at various periods $P_I = 14$, 30 and 60 s without applying external magnetic field ($H = 0$). The upper part in Fig. 1 is a schematic diagram of the time dependence of the driving current. The sample voltage response to the SW current evolves in the shape of regular sinusoidal voltage oscillations for all periods, except the one for $P_I = 60$ s. Figure 1c — the V–t curve, measured for SW current with period $P_I = 30$ s, exhibits oscillations resembling the variation of SW current with time (Fig. 1a). The voltage oscillations amplitude increases by increasing the period P_I, due to relaxation effects involving during the process. Moreover, the difference between the periods of the SW current drive and sample voltage response is negligibly small, this can cause a differences in the phase between them.

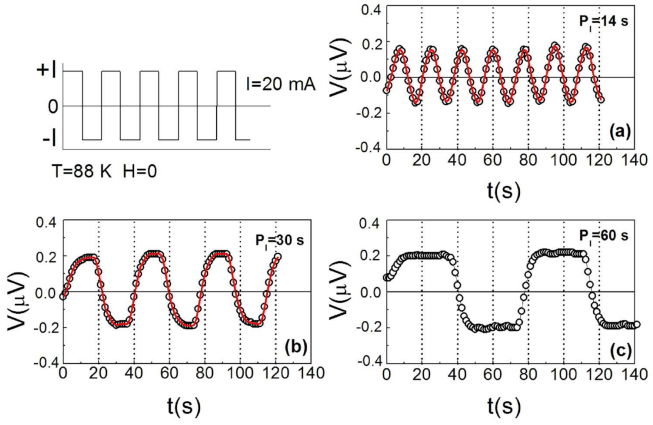

Fig. 1. Time evolution of the sample voltage measured for a SW current with amplitude $I = 20$ mA and period P_I: (a) 10 s, (b) 15 s, and (c) 30 s. The measurements were made at $T = 88$ K and $H = 0$. The top part shows schematically the SW current applied to the sample.

Due to the SW current, the oscillatory driving force can cause a coherent motion of flux lines along weak pinning centers, and, after the forth and back repetitive oscillations, the flux line system becomes spatially more ordered in time. The regular voltage oscillations, without observation of any instability (i.e., voltage jumps or drops) or noise, evince for the formation of this ordered state. The voltage response associated with voltage oscillations lies typically in the range of 10^{-6}–10^{-7} V [2, 5, 8]. This suggests that total number of the flux lines contributing to the oscillations is nearly constant and the change in the measured voltage can be related to the periodic variations in the average velocity of flux lines. The repetitive voltage oscillations seen in the V–t curves of the YBCO/Ag sample (Fig. 1) are quite smooth and no voltage drop or jump are observed for the negative or positive periods of SW drive. We suggest that the current-induced flux lines fluctuate between the ordered and disordered states by subjecting the same pinning forces in average.

The voltage oscillations in the YBCO/Ag sample can be described by an Eq. (1) given in experimental part. The red colored bold solid lines in Figs. 1,2 are the best fits of Eq. (1) to the experimental data. We note that the fitting procedure was performed for each period of repetitive voltage oscillations separately. As it is seen from the V–t curves given in corresponding figures, there is a qualitative concordance between the experimental data and calculated theoretical curves (red colored bold solid lines). Further, the curve fitting shows that the phase angle (φ) has different values for the observed iterative voltage oscillations. The grid lines is useful way for monitoring these differences in the phase angles. Table I shows the values of phase angle φ found from the experimental V–t data given in Fig. 1. The phase angle φ takes negative values for all period values of SW current and tends to decrease from first period to the final one.

TABLE I

The phase angles φ obtained by fitting Eq. (1) to the V–t data in Fig. 1 ($T = 88$ K, $H = 0$ mT, $I = 20$ mA).

Periodof response (P) of response (P)	Phase angle (φ)	
	SW $P_i = 14$ s	SW $P_i = 30$ s
P_1	$-1.20\pi/2$	$-0.52\pi/2$
P_2	$-1.00\pi/2$	$-0.56\pi/2$
P_3	$-1.20\pi/2$	$-0.56\pi/2$
P_4	$-1.46\pi/2$	–
P_5	$-1.64\pi/2$	–
P_6	$-1.88\pi/2$	–
P_7	$-2.08\pi/2$	–

The effect of the magnetic field (H) on the the voltage oscillations is demonstrated in Fig. 2. The measurements were performed at $T = 88$ K for external magnetic fields of $H = 10$, 16, and 20 mT. The amplitude and period of the SW current were $I = 10$ mA and $P_I = 20$ s, respectively. The V–t curve measured at $H = 10$ mT exhibits sinusoidal-type regular voltage oscillations (Fig. 2a). However, the line shape of the oscillations in the V–t curves measured for $H = 14$ and 16 mT differs from that measured for $H = 10$ mT. Figure 2b and c demonstrates dissipation in the early stage of the voltage response, then as the time progresses, the oscillations change their character. The first voltage jump (or drop) occurs at ≈ 12 s and 11 s on the V–t curves measured at $H = 16$ mT and $H = 20$ mT, respectively.

After the time values, where the voltage jump (or drop) occurred, the time variation of the voltage response of the sample (with a relatively larger amplitude of ≈ 0.5 μV) resembles the line shape of the SW current.

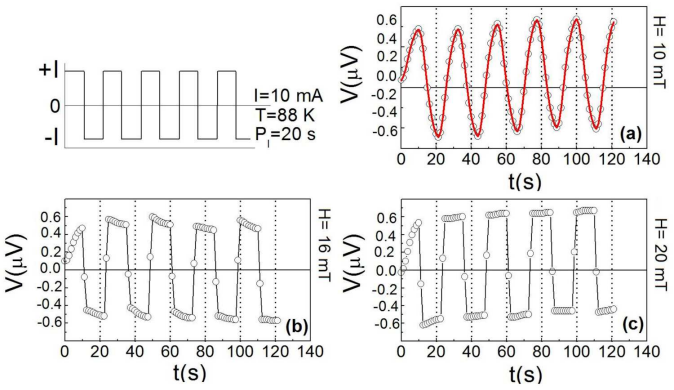

Fig. 2. Time evolution of the sample voltage measured for SW current (with amplitude $I = 10$ mA and period $P_I = 10$ s) at $T = 88$ K and external magnetic fields: (a) $H = 10$ mT, (b) $H = 16$ mT, and (c) $H = 20$ mT. The top part shows schematically SW current.

Another important parameter in the observation of voltage oscillations is the magnitude of applied magnetic field. It is seen from the V–t curves in Fig. 2b and Fig. 2c that the external magnetic field causes a change in the form of voltage oscillations, and the oscillations undergo a significant change due to the increase in magnetic field. The sharp rise in the sample voltage after dissipation can be due to sudden increase in the fraction of the moving flux lines. By the increasing field, flux lines ready to move and try to penetrate continuously into the grains. Note that the first voltage drop occurs at ≈ 12 s and ≈ 11 s for $H = 16$ mT and $H = 20$ mT, respectively (see Fig. 2b and c). The difference can be attributed that effective Lorentz force on flux lines increases, as the magnitude of external magnetic field is increased from 16 mT to 20 mT.

However, the best fits of Eq. (1) to the experimental V–t data in Fig. 2 are obtained when the phase angle φ takes approximately constant values for each period of response (Table II). This implies that the phase angle φ does not change much in time along the whole relaxation process. It is seen from the Table II that the value of the phase angle φ is essentially nearly constant of the applied magnetic field. The physical descriptions is as follows. The order parameter in the intergranular region of the YBCO/Ag sample is easily suppressed by the external magnetic field and some of the flux lines penetrate into the grains along the easy motion channels and some of them are pinned inside the grains. We note that, in the presence of external magnetic field and at this temperature ($T = 88$ K), the grains are not fully superconducting islands. Therefore, the motion of flux lines can give a regular and ordered response to the change in the polarity of SW current, and, thus, the initial and final conditions in preparing the flux line system corresponding to each cycle can remain nearly constant in time.

TABLE II

The phase angles φ obtained by fitting Eq. (1) to the V–t data in Fig. 2 ($T = 88$ K, SW $P_i = 10$ s, $I = 10$ mA).

Period of response (P) of response (P)	Phase angle (φ) $H = 10$ mT
P_1	$-0.32\pi/2$
P_2	$-0.34\pi/2$
P_3	$-0.32\pi/2$
P_4	$-0.30\pi/2$
P_5	$-0.28\pi/2$

The V–t curves in Figs. 1 and 2 also demonstrate that the voltage oscillations are quite symmetric and follow the polarity change of the SW drive. Since we used symmetric SW currents, there should be an equality between flux exit and flux entry during regular oscillations of flux lines (or current induced flux lines).

Kalisky et al. [12] observed peculiar spatiotemporal oscillations in the vortex matter of single crystalline sample of $Bi_2Sr_2CaCu_2O_{8+x}$ (BSCCO) generated in the absence of external ac magnetic field. Oscillatory behavior in space and time of the magnetic induction has been explained in terms of flux wave phenomenon which appears near the order-disorder phase transition under suitable conditions. Barness et al. [13, 14] pointed out that the oscillatory temporal relaxation observed in single crystalline sample of BSCCO involves ordinary flux creep and annealing transient vortex states. It is assumed that the magnetic diffusion equation governs the relaxation process evolving in the BSCCO sample. The magnetic diffusion equation can be described by the Maxwell equations

$$\partial B/\partial x = -\mu_0 J, \tag{2}$$

where J is the current density and μ_0 is the magnetic permeability of free space, and

$$\partial B/\partial t = -\partial E/\partial t, \tag{3}$$

where $E = R_F J \exp(-U/k_B T)$ is the electric field, $R_F = R_N(B/B_{c2})$ is the flux flow resistivity, and U is the pinning potential [10–12]. Assuming a logarithmic current density (J) dependence of U,

$$U(J) = U_0 \ln\left(\frac{J_c}{J}\right), \tag{4}$$

one can get easily

$$\frac{\partial B}{\partial t} = \frac{1}{\mu_0}\frac{\partial}{\partial x}\left(D_f \frac{\partial B}{\partial x}\right) \tag{5}$$

for the relaxation process in one dimension [12–14]. Here $D_f = R_F(J/J_c)^n$ is the diffusion coefficient with $n = U_0/k_B T$. Barness et al. [13] showed that, under suitable conditions, the coupling between the annealing of disordered state and conventional flux creep could produce the oscillatory behavior of magnetic induction in time. Their experimental studies reveal that the oscillations appearing in magnetic induction can be related to periodic transformations in the vortex matter between ordered and disordered states.

A similar analysis can be done for the electric diffusion equation and the same Maxwell equations (Eq. (2) and Eq. (3)) can be reduced to

$$\frac{\partial E}{\partial t} = f(E)\frac{\partial^2 E}{\partial x^2}, \tag{6}$$

where $f(E) = \frac{1}{\mu_0}(\frac{\partial E}{\partial J})$. In this case, we suggest that combination of electric diffusion equation with conventional flux creep theory and the logarithmic current dependence of pinning potential can give similar time dependent oscillatory behavior of electric field (or voltage) for the time intervals responds to the positive and negative cycles of the SW current with long P_I values, i.e., $0 \leq t < P_I/2$, and $P_I/2 \leq t < P_I$, respectively.

4. Relationship between voltage oscillations and charge density waves

Silver redistributes itself along grain boundaries forming metallic amorphous regions between grains. On the other hand, surface imperfections can be considered as "surface weak links" which prevents the penetration of flux lines from the outer of sample. It is naturally expected that surface weak links in different size is also affected by adding of Ag since the distribution of Ag covers the whole bulk sample. Thus, the flux lines can easily penetrate along metallic regions embedded surface weak links.

The oscillations of voltage response generally follow the period of the SW current. Typical examples for the FFT obtained from Fig. 1a,b are shown in Fig. 3a,b. The fundamental periods ($P_{V_{osc},FFT}$) are found as 14.08 s and 29.76 s, which are in good agreement with the periods of the SW drive, i.e., $P_I = 14$ and 30 s, respectively. The regular voltage oscillations may be described as the dissemination of fluctuations of vortex density [2, 7, 8]. It has been suggested that the system of weakly pinned vortices resembles the pinned CDW state. Experimental results on charge density waves gives that coherent current or voltage oscillations appear along the sample after reaching the threshold value of the driving voltage or current [15–19]. In the present study, we suppose that a physical mechanism regarding the density instabilities of flux lines (or self magnetic field (SMF) lines) can be introduced as a possible mechanism for coherent voltage oscillations. Such coherent density fluctuations of flux lines (or SMF lines) can develop along the YBCO/Ag sample and can result in similar effects as in the CDW's situation.

5. Conclusion

The effect of applied square wave current on V–t curves as functions of the period of the SW current were investigated at external magnetic fields. The nonlinear voltage behavior in the time evolution of the voltage curves V–t to the SW current with proper periods or proper amplitude of the SW current shows itself as sinusoidal voltage oscillations, which were mainly discussed due to of the dynamic competition between pinning and de-pinning mechanism.

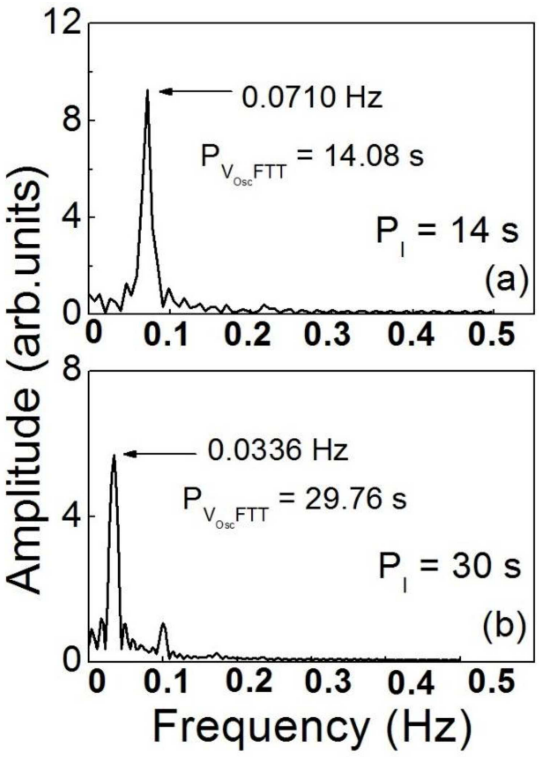

Fig. 3. FFT of the V–t curves given in Fig. 1a–c. The fundamental frequency is marked on each curve. The fundamental period $P_{V_{osc},FFT}$ found from FFTs is given for each curve with the period of applied SW currents.

This dynamic competition of flux lines causes an enhancement or suppression in the superconducting order parameter depending on the magnitude of the driving current and the coupling strength of weak-link structure with the chemical and anisotropic states of the sample.

Due to SW current, the oscillatory driving force can cause relatively a coherent motion of flux lines along weak pinning centers, after forth and back repetitive oscillations. There is a symmetry with respect to the zero in voltage oscillations. We conclude that the existence of the elastic coupling between pinning centers and flux lines in the grain boundaries, partially inside the grains. This situation was also correlated to the same amount of the flux entry and leaving along the YBCO/Ag sample during time evolution of the voltage (refers to coherent voltage oscillations). By increasing the period of the applied current, voltage oscillation changes to the line shape of SW current in time. It means that the Lorentz force increases and it dominates the pinning force so depinning wins mostly this competition.

It was shown that the voltage oscillations can be described well by an empirical expression $V(t) \approx \sin(\omega t + \varphi)$ (see Eq. (1)). We found that the phase angle φ generally takes different values for the repetitive oscillations. We suggest that, for each cycle observed, the initial conditions of the flux lines joining the motion are determined by the distribution of flux lines formed by the former cycle and, thus, every cycle prepares new initial condition

for the next cycle. Therefore, it is natural to expect such phase difference between successive oscillations.

The presence of Ag between the YBCO-123 grains can provide a plastic flow region and relax undesirable residual stresses in the ceramic sample resulting from the grain anisotropy of superconductors. We suggest that doping of Ag destroys partly the intergranular pinning properties of the YBCO ceramic by increasing the grain coupling. Transport measurements, at low dissipation levels, the flux lines enter into the intergranular region after overcoming the surface weak-links and demagnetizing factor of the sample. It is expected that the presence of metallic regions (or paths) formed by Ag atoms along grain boundaries act as easy motion channels for flux lines. Thus, the flux lines can move easily in those regions without encountering any obstruction until they meet the pinning centers or superconducting grains.

Fast Fourier transform analysis of the observed voltage oscillations showed that the oscillation period is comparable to that (P_I) of the SW current and approximately the same. This finding suggests a physical mechanism associated with charge density waves. In fact, this weakly pinned flux line system in YBCO/Ag similar to the general behavior of charge density waves. In addition, since converting the SW current to sinusoidal voltage oscillations, the silver doped YBCO sample behaves like a double-integrator at certain values of period, SW current, magnetic field and temperature.

References

[1] G. D'anna, P. Gammel, H. Safar, G. Alers, D. Bishop, J. Giapintzakis, D. Ginsberg, *Phys. Rev. Lett.* **75**, 3521 (1995).

[2] S. Gordeev, P. De Groot, M. Oussena, A. Volkozub, S. Pinfold, R. Langan, R. Gagnon, L. Taillefer, *Nature* **385**, 324 (1997).

[3] A. Altinkok, H. Yetiş, K. Kiliç, A. Kiliç, M. Olutaş, *Physica C Superconduct.* **468**, 1419 (2008).

[4] W. Henderson, E. Andrei, M. Higgins, *Phys. Rev. Lett.* **81**, 2352 (1998).

[5] K. Kiliç, A. Kiliç, A. Altınkök, H. Yetiş, O. Çetin, *Europ. Phys. J. B Condens. Matter Complex Syst.* **48**, 189 (2005).

[6] W.K. Kwok, G.W. Crabtree, J.A. Fendrich, L.M. Paulius, *Physica C Superconduct.* **293**, 111 (1997).

[7] S. Gordeev, P. de Groot, M. Oussena, R. Langan, A. Rassau, R. Gagnon, L. Taillefer, *Physica C Superconduct. Its Appl.* **282**, 2033 (1997).

[8] A. Rassau, S. Gordeev, P. de Groot, R. Gagnon, L. Taillefer, *Physica C Superconduct.* **328**, 14 (1999).

[9] E. Govea-Alcaide, I. García-Fornaris, P. Suzuki, R. Jardim, *J. Superconduct. Novel Magn.* **29**, 2783 (2016).

[10] A. Altinkok, K. Kiliç, M. Olutaş, A. Kiliç, *J. Superconduct. Novel Magn.* **27**, 651 (2014).

[11] A. Altinkok, K. Kiliç, M. Olutaş, A. Kiliç, *J. Superconduct. Novel Magn.* **26**, 3085 (2013).

[12] B. Kalisky, M. Gitterman, B.Y. Shapiro, I. Shapiro, A. Shaulov, T. Tamegai, Y. Yeshurun, *Phys. Rev. Lett.* **98**, 017001 (2007).

[13] D. Barness, I. Sochnikov, B. Kalisky, A. Shaulov, Y. Yeshurun, *Physica C Superconduct.* **468**, 280 (2008).

[14] D. Barness, M. Sinvani, A. Shaulov, C. Trautmann, T. Tamegai, Y. Yeshurun, *J. Appl. Phys.* **105**, 07E310 (2009).

[15] H. Jin, H.-H. Wen, H.-P. Yang, Z.-Y. Liu, Z.-A. Ren, G.-C. Che, Z.-X. Zhao, *Appl. Phys. Lett.* **83**, 2626 (2003).

[16] K. Ringland, A. Finnefrock, Y. Li, J. Brock, S. Lemay, R. Thorne, *Phys. Rev. Lett.* **82**, 1923 (1999).

[17] D. Mtsuko, D. Churochkin, S. Bhattacharyya, *MEMS Electro-Optic Syst.* **10036**, 1003606 (2017).

[18] Z. Jing, H. Yong, Y. Zhou, *Supercond. Sci. Technol.* **29**, 105001 (2016).

[19] Z. Jing, H. Yong, Y.-H. Zhou, *Supercond. Sci. Technol.* **28**, 075012 (2015).